Time and Space Transition of DC Electric Field Distribution Based on Emerging Field by Accumulated Charge in Gas-solid Composite Insulation Structure

Ryuichi Nakane and **Naoki Hayakawa**
Department of Electrical Engineering, Nagoya University
Furo-cho, Chikusa-ku, Nagoya 464-8603, Japan

Hitoshi Okubo
Department of Electrical Engineering, Aichi Institute of Technology
1247 Yachigusa, Yakusa-cho, Toyota 470-0392, Japan

ABSTRACT

In this paper, we investigate the time and space transition characteristics of DC electric field stress in SF_6 gas from the initial state DC-on to final DC steady-state in gas-solid composite insulation systems. Using a simple rod-electrode configuration and actual insulating epoxy-spacer model, the electric field distributions of the epoxy-spacer in SF_6 gas and time constant τ of electric field formation from DC-on to DC steady-state are calculated under DC voltage based on the electric conduction characteristics, that is, the source of charge carrier. In addition, the emerging electric field distributions due to accumulated charge on solid insulator surface are introduced to elucidate the time transition process of electric field stress in the gap space between HV conductor and GND from DC-on to DC steady-state quantitatively. As a result, we quantitatively clarify that the time constant τ of electric field formation from DC-on to DC steady-state are highly dependent on the non-uniform factor η and location of the gap space in the electrode configuration under non-uniform DC electric field. The locations with higher electric field stress in the gap space have the shorter time constant τ. In addition, the time transition process of electric field stress in SF_6 gas depends on the gap space and the location of maximum electric field change during time transition. Especially, we clarify that the highest electric field stress in SF_6 gas may emerge in actual GIS structure from DC-on to DC steady-state based on the time transition process of emerging electric field due to accumulated charge.

Index Terms — **HVDC insulation, DC-GIS, charge accumulation, electric field distribution, time constant, gas-solid composite insulation.**

1 INTRODUCTION

It is necessary to improve the reliability of HVDC power equipment such as SF_6 gas insulated switchgear (GIS) for the introduction of long distance power transmission and the integration of renewable energy systems [1]. Especially, the enhancement of electrical insulation performance in DC gas insulated switchgear (DC-GIS) leads to advantages such as space saving installations and maintaining reliability.

The electric field distributions in DC-GIS are entirely different from those of the AC application [2]. In the case of gas-solid composite insulation systems under DC voltage, the electric field stresses in SF_6 gas are characterized by the charge accumulation at the interface between the epoxy-spacer and SF_6 gas [3-5]. Hence, DC charging phenomena, which depend on the conductivity values of the materials of gas and epoxy-spacer, will be one of the critical parameter to be investigated. However, the conductivity values of materials in GIS are not so easily identified, as they are influenced by factors such as the surrounding temperature, electric field stress and moisture content [6, 7]. Especially, the conductivity in SF_6 gas would be determined by the local existence of the source of charge carrier such as the surface roughness of the conductor, impurities, and partial discharges [8, 9]. In particular, DC electric field stresses in gas are forced to be changed and distorted depending on the charging process and the location in the field space during the time transition from the initial state to DC steady-state [4]. Therefore, in order to better understand the distortion process of DC electric field distributions, it is required to quantitatively investigate the time transition of the electric field generated by the accumulated

Manuscript received on X Month 2005, in final form XX Month 2005.

charge on the solid insulator. On the other hand, few studies have reported the electric field distribution generated by the accumulated charge in detail.

In this paper, the electric field distributions and time constant τ from the initial state DC-on to final DC steady-state in gas-solid composite insulation systems were calculated and discussed. Using a simulation model with simple axisymmetric 3D rod-electrode configuration and an actual insulating epoxy-spacer model, the time transition characteristics of DC electric field stress in SF_6 gas were investigated based on the charge activity on the solid insulator. Especially, the electric field generated by the accumulated charge on solid insulator surface are introduced to elucidate the time transition process of electric field stress in the gap space between HV conductor and GND during time transition. Note that, we represent "the electric field generated by the accumulated charge on the solid insulator" as "the emerging field" in this paper.

2 DC ELECTRIC FIELD ANALYSIS METHOD IN COMPOSITE INSULATION SYSTEMS

2.1 TIME TRANSITION OF DC ELECTRIC FIELD DISTRIBUTION AND CHARGE ACCUMULATION FROM DC-ON TO DC STEADY-STATE

The DC electric field distribution $\boldsymbol{E}_{\mathrm{DC}}$ is dependent on the permittivity and electric conductivity of the insulating materials such as SF_6 gas and epoxy-spacer. That is, the following equation (1) based on Gauss's law is to be solved [10].

$$\mathrm{div}\left(\sigma + \frac{\mathrm{d}}{\mathrm{dt}}\varepsilon\right)\boldsymbol{E}_{\mathrm{DC}} = 0 \qquad (1)$$

Where ε: permittivity of insulating material, σ: electric conductivity. From equation (1), at initial capacitive state, the electric field (DC-on) is determined by the permittivity ε of the insulating materials. From DC-on to DC steady-state, the electric field distributions are forcibly changed based on equation (1). Under DC steady-state conditions, the DC electric field distribution is finally determined by the electric conductivity σ of the insulating materials.

The charge accumulation under DC application is calculated by the following equation (2) at the interface between SF_6 gas and epoxy-spacer.

$$-\varepsilon_{\mathrm{gas}}\boldsymbol{E}_{\mathrm{gasn}} + \varepsilon_{\mathrm{EP}}\boldsymbol{E}_{\mathrm{EPn}} = -q \qquad (2)$$

Where $\boldsymbol{E}_{\mathrm{gasn}}$: the normal component of the total electric field stress to the insulator surface in SF_6 gas, $\boldsymbol{E}_{\mathrm{EPn}}$: the normal component of the total electric field stress to the insulator surface in epoxy-spacer, q: surface charge density at the interface.

2.2 CHARGE CARRIER SUPPLY SOURCE AND CHARGE BEHAVIOR AROUND EPOXY-SPACER IN SF_6 GAS

Figure 1 shows the schematic model of DC charge activity in gas-solid composite insulation. The conductivity values of the epoxy-spacer and gas depend on the state of electrode roughness, microscopic protrusions and other sources of charge carrier. In the case of insulation conditions without any defects, the conduction process in solids would be predominant, that is, (a) solid-dominant conditions ($\sigma_{EP} > \sigma_{gas}$). On the other hand, in the case of insulation defect, for example with metallic particles and protrusions, partial discharge could be generated and DC electric field distributions are quickly distorted by charging phenomena through the charge carrier in SF_6 gas, i.e., (b) gas-dominant conditions ($\sigma_{EP} < \sigma_{gas}$) [8, 11-14].

In one example, Figure 2 shows the calculated 5% equi-potential line and the conductivity distribution in SF_6 gas for an actual insulating epoxy-spacer model, assuming the main source of charge carrier is only natural ionization by cosmic ray. The conductivity in SF_6 gas in Figure 2 is calculated based on transport equation of positive and negative ion including the

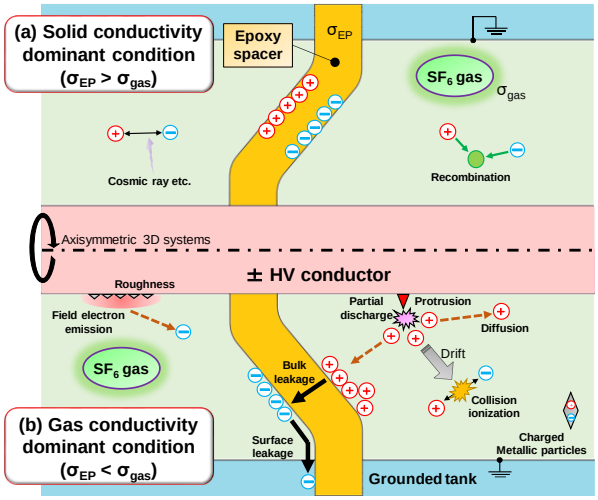

Figure 1. Charge carrier supply sources and charge behavior under HVDC conditions in gas-solid composite insulation systems.

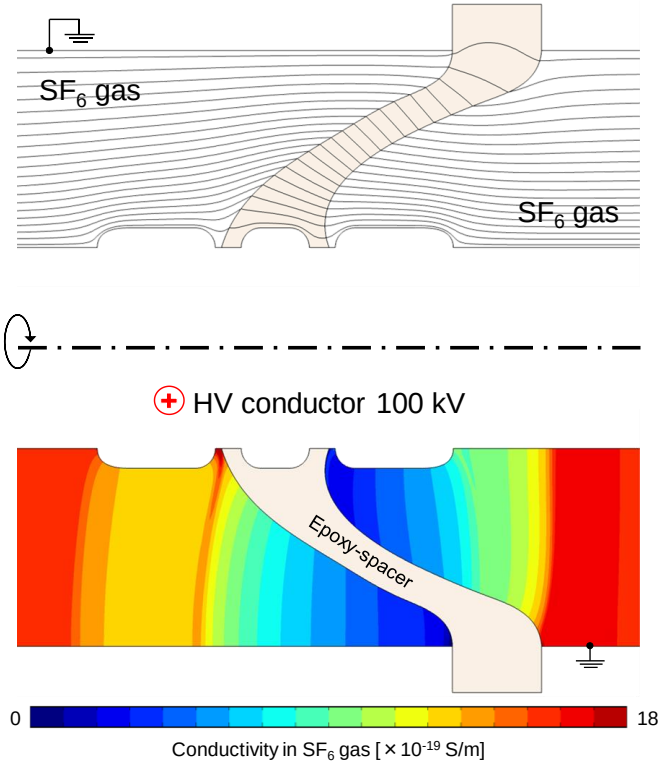

Figure 2. 5% equi-potential line (upper figure) and conductivity in SF_6 gas (lower figure) around actual insulating epoxy-spacer model (id of outer sheath Φ450, od of inner HV conductor Φ150 mm, +DC 100 kV application, 0.5 MPa-abs).

terms of ion pair generation, recombination, drift due to electric field and diffusion [5]. From these results, in Figure 2, we can find that the location and the shape of the spacer would affect the electric field distribution and th e local distribution of gas conductivity. The conductivity distributions in SF_6 gas are not uniform and depending on the gap space. The values of conductivity in SF_6 gas range from 10^{-19} to 10^{-18} S/m. However, this electric field and conductivity distributions in SF_6 gas are under the conditions in which the influences of the surface roughness of HV conductor, charge injection from electrodes and partial discharge due to protrusions are negligible. Therefore, the actual conductive characteristics in SF_6 gas contributing to the charge accumulation on the solid insulator and DC electric field distribution are not so easily identified quantitatively.

In this paper, in order to distinguish gas-conductivity-dominant conditions (a higher conductivity value in SF_6 gas than that in epoxy-spacer) and solid-conductivity-dominant conditions (a higher conductivity value in epoxy-spacer than that in SF_6 gas), we use a conductivity ratio between solid and gas as the parameter equivalently corresponding to the change of state of charge carrier.

3 SIMPLE GAS-SOLID COMPOSITE INSULATION MODEL

3.1 TIME TRANSITION CHARACTERISTICS OF ELECTRIC FIELD STRESS

Firstly, in order to make the time dependent characteristics clearly understandable, a simulation model with simple axisymmetric 3D rod-electrode configuration systems in gas-solid composite insulation was introduced, as shown in Figure 3. The aim of the introduction of a simulation model shown in Figure 3 is to show the relationship between the emerging electric field and the resultant DC electric field clearly while changing the shape of the rod-electrode under non-uniform electric field. We investigate the time and gap space dependent characteristics of DC electric field with non-uniformity factor η as a parameter. The conductivity $\sigma_{EP} = 10^{-17}$ S/m of epoxy-spacer and $\sigma_{gas} = 10^{-19}$ - 10^{-16} S/m of SF_6 gas are given [5, 7, 13].

Figure 4 shows the time transition of the electric field stress in SF_6 gas at each Point a - c on the rod-electrode for Model 1. The electric field is relaxed by the charge accumulation on the solid insulator over time. In particular, at DC-on (t = 0 [h]), the electric field stress at Point a shows the maximum value, whereas after t = 500 [h], the electric field stress at Point b shows the maximum value. This means that the locations of the maximum electric field stress in SF_6 gas are changed over time and the time constant at different location on the electrode surface, as well.

Figure 5 shows the time constant τ of the electric field in SF_6 gas from DC-on to DC steady-state along the rod-electrode surface ℓ while changing the tip curvature radius r (non-uniformity factor η = 1.24 - 4.20, Model 1 - Model 3) in comparison with the parallel plane electrode model (η = 1.00). From this figure, the time constant τ of the electric field in SF_6 gas are dependent on the locations of the gap space under "non-uniform" electric field. In addition, the larger the non-uniformity factor η and the conductivity ratio σ_{EP}/σ_{gas}, the longer time constant τ of changing electric field in SF_6.

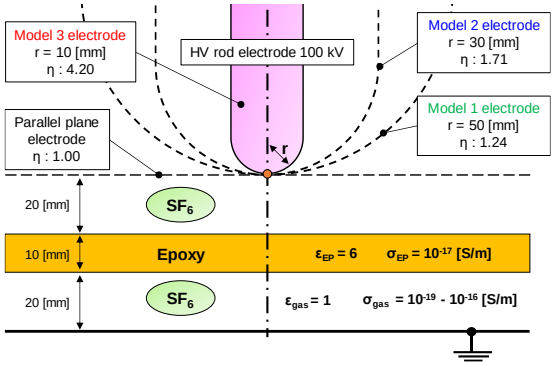

Figure 3. Simulation model of DC transient electric field in gas-solid composite insulation.

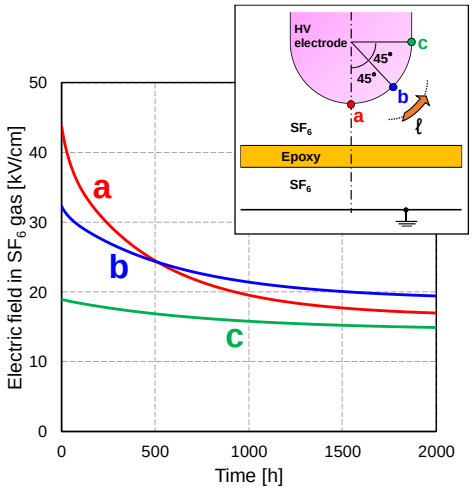

Figure 4. Time transition of DC electric field stress in SF_6 gas on the different location of HV rod-electrode surface for Model 1 (σ_{EP}/σ_{gas} = $10^{-17}/10^{-16}$).

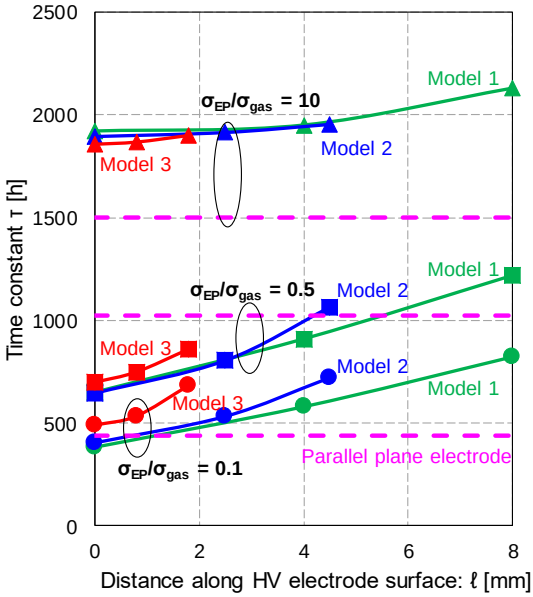

Figure 5. Time constant τ of DC electric field transition in SF_6 gas on HV rod-electrode surface.

3.2 TIME TRANSITION CHARACTERISTICS OF EMERGING ELECTRIC FIELD DUE TO ACCUMULATED CHARGE

Figure 6 shows the time transition of the emerging field due to the accumulated charges on the solid insulator (left side) and the resultant synthetic electric field stress distributions in SF_6 gas (right side) for Model 1. The emerging field $\boldsymbol{E}_c$ distributions due to the charge accumulation are calculated by the following equation (3).

$$\boldsymbol{E}_{\mathbf{DC}} = \boldsymbol{E}_{\mathbf{a}} + \boldsymbol{E}_{\mathbf{c}} \tag{3}$$

Where $\boldsymbol{E}_a$: capacitive electric field at DC-on, $\boldsymbol{E}_{DC}$: synthetic electric field from DC-on to DC steady-state.

The emerging field due to positive potential is expressed by red color filled and negative potential is blue color filled. From these figures, in the case after 100 [h], the synthetic electric field in SF_6 gas is mainly concentrated at the rod-electrode tip surface. On the other hand, the synthetic electric field in SF_6 gas is relaxed corresponding to the emerging field during the time transition. First of all, the emerging electric field is distributed around at the rod-electrode tip, Point a, after 100 [h]. Finally, the emerging electric field progress in the direction of Point b and c during time transition. This means that the location of the maximum electric field in SF_6 gas transits from DC-on to DC steady-state as shown in Figure 4.

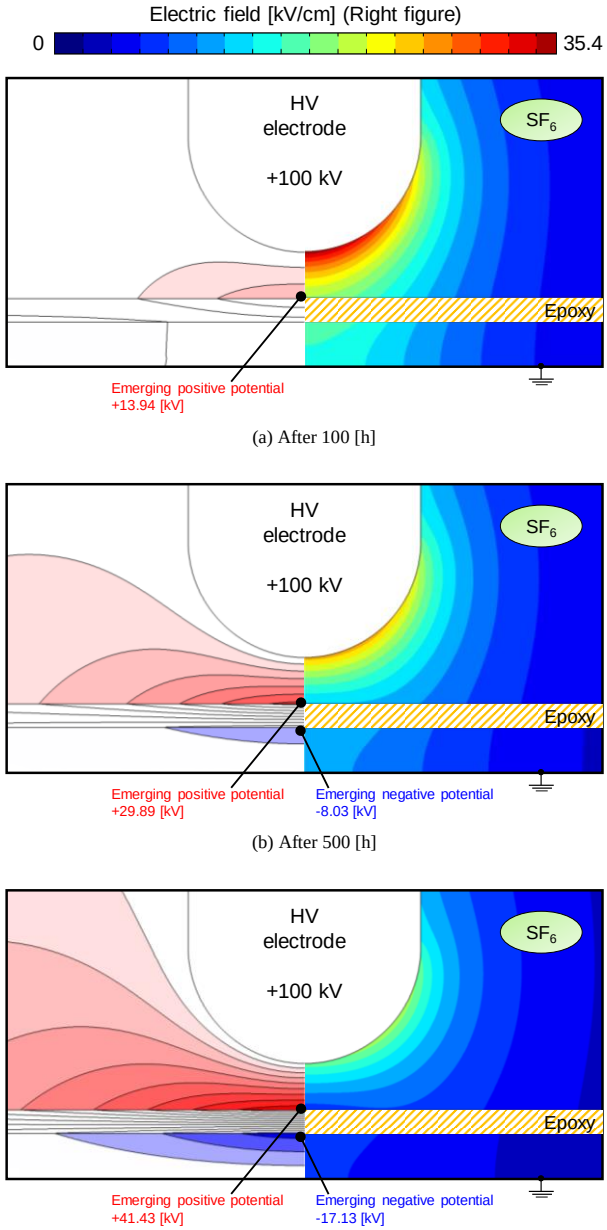

Figure 6. Emerging field $\boldsymbol{E}_c$ (left figure) and synthetic electric field $\boldsymbol{E}_{DC}$ (right figure) distributions for Model 1 ($\sigma_{EP}/\sigma_{gas} = 10^{-17}/10^{-16}$).

As a result, we found that the time transition characteristics of DC electric field stress in SF_6 gas depends on the location of the gap space and the location of the maximum electric field stress may change over time. This is because the emerging field due to the accumulated charge on the solid insulator progress during time transition. In addition, the smaller conductivity ratio σ_{EP}/σ_{gas}, the shorter time constant from DC-on to DC steady-state. The time constant tends to be short at the location of electric field concentration such as Point a.

4 ACTUAL INSULATING GAS AND EPOXY-SPACER MODEL

4.1 ELECTRIC FIELD DISTRIBUTION

In this section, we investigate the time transition process of the accumulated charge and resultant DC electric field distribution depending on the location by using an actual GIS structure based on the previous section. Figure 7b shows the electrode configuration of an actual insulating epoxy-spacer model with a coaxial electrode system and solid insulator in SF_6 gas. Figure 7a shows the electric field distribution at DC-on,

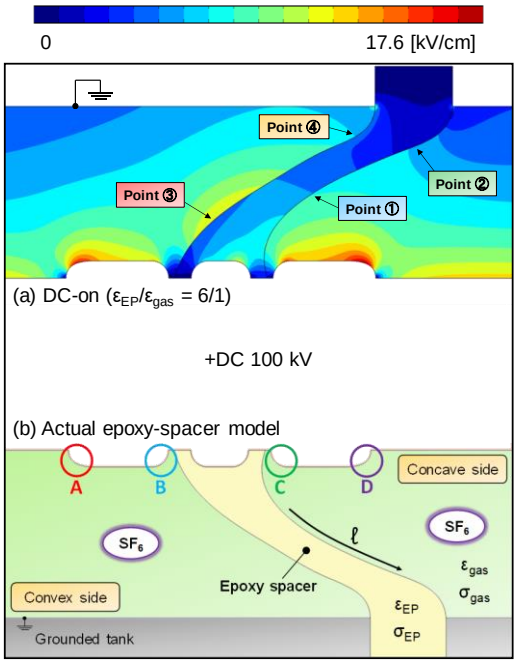

Figure 7. Actual epoxy-spacer model in gas-solid composite insulation systems (lower figure, id of outer sheath Φ450, od of inner HV conductor Φ150 [mm], +DC 100 [kV] application) and electric field distribution at DC-on (upper figure, $\varepsilon_{EP}/\varepsilon_{gas}$ = 6/1).

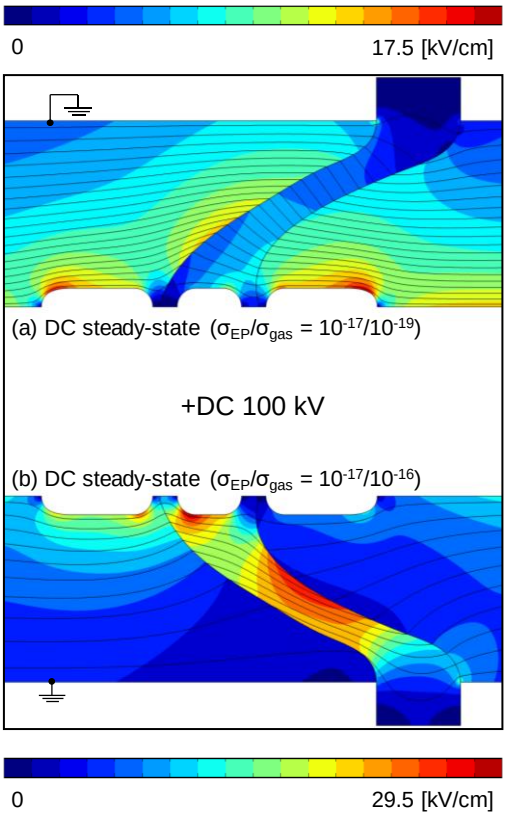

Figure 8. Electric field distributions under DC steady-state ($\varepsilon_{EP}/\varepsilon_{gas}$ = 6/1, $\sigma_{EP} = 10^{-17}$, $\sigma_{gas} = 10^{-16}$ (upper figure) and 10^{-19} (lower figure) [S/m]).

capacitive field. The electric field stress is mainly concentrated around the HV conductor shield surface at Point A and D in SF_6 gas.

Figure 8 shows the electric field distributions and 5% equi-potential lines under DC steady-state, resistive field, in the case of gas-dominant conditions ((a) upper figure, $\sigma_{EP} < \sigma_{gas}$) and solid-dominant conditions ((b) lower figure, $\sigma_{EP} > \sigma_{gas}$). Firstly, the electric field distribution under DC steady-state in the case of gas-dominant conditions ($\sigma_{EP} < \sigma_{gas}$) is entirely different from that at DC-on. In the case of DC steady-state under gas-dominant conditions ($\sigma_{EP} < \sigma_{gas}$), the electric field stress is mainly concentrated inside the epoxy-spacer. Especially, the location of the maximum electric field stress in SF_6 gas shifts from Point A and D to Point B on the HV conductor shield.

On the other hand, the electric field distribution under DC steady-state under solid-dominant conditions shows almost the same characteristics as with DC-on. These characteristics of the electric field distributions are due to the fact that the value of conductivity of SF_6 gas is greatly dependent on the source of charge carrier and the charge accumulation process on the solid insulator surface under DC voltage application.

4.2 CHARGE DENSITY DISTRIBUTIONS ON EPOXY-SPACER SURFACE UNDER DC VOLTAGE

Figure 9 shows the charge density distributions along the spacer creepage length ℓ under DC steady-state on both the concave and convex sides. In the case of gas-dominant conditions (σ_{EP}/σ_{gas} = 0.5 - 0.1), positive charges are accumulated on the concave side and negative charges on the convex side, as shown in Figure 1b under positive DC voltage application. On the other hand, in the case of solid-dominant conditions (σ_{EP}/σ_{gas} = 10 - 100), negative charges are accumulated on the concave side and positive charges on the convex side, as shown in Figure 1a under positive DC voltage application. These charge polarities and amount characteristics may strongly depend on the electrical conduction characteristics of gas-solid composite insulation, that is, on the type of the source of charge carrier. In the case of gas-dominant conditions ($\sigma_{EP} < \sigma_{gas}$), the main source of charge carrier is expected to be ionization by partial discharge in high electric field region, while in the case of solid-dominant conditions ($\sigma_{EP} > \sigma_{gas}$), from the inside of the epoxy-spacer. Therefore, in the case of gas-dominant conditions, DC electric field distributions could be greatly distorted by remarkable charge accumulation on the epoxy-spacer as shown in Figure 8.

Figure 10 shows the time dependent characteristics of the charge density distributions along the spacer creepage length ℓ under gas-dominant conditions ($\sigma_{EP} < \sigma_{gas}$) on both the concave and convex sides from DC-on to 300 [h]. The amount of charge density on the epoxy- spacer surface is built up during the time transition on both the concave and convex sides. On the concave side, the charge density during the time transition from DC-on to DC steady-state shows almost the same shape of

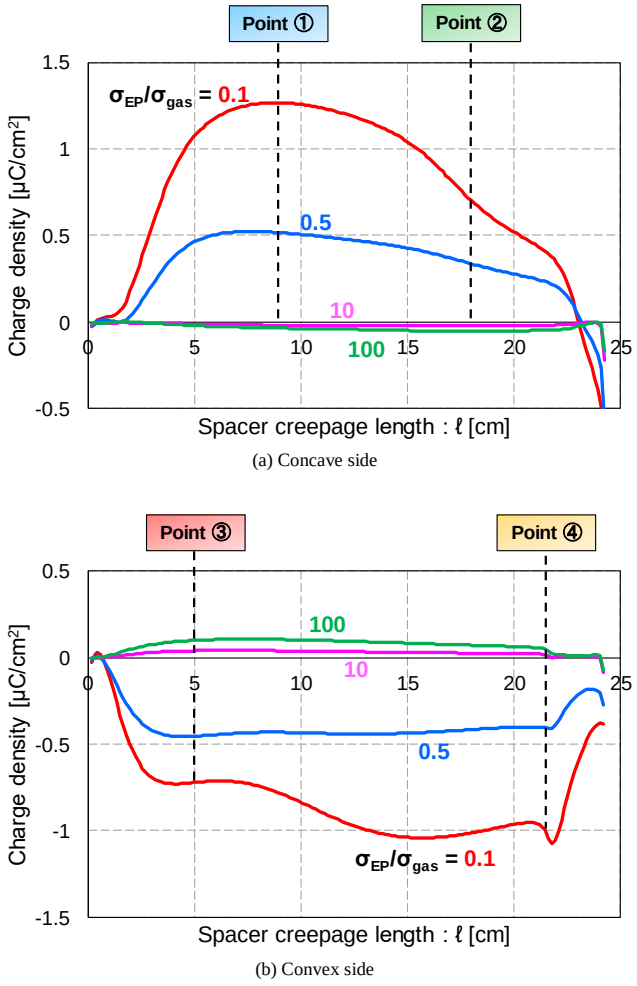

Figure 9. Charge density distributions under DC steady-state along spacer creepage length ℓ while changing conductivity ratio σ_{EP}/σ_{gas} ($\varepsilon_{EP}/\varepsilon_{gas}$ = 6/1, $\sigma_{EP} = 10^{-17}$, $\sigma_{gas} = 10^{-19}$ - 10^{-16} [S/m], +DC 100 kV application).

distributions, which indicates a peak value around Point 1, as shown in Figure 9a and 10a. On the other hand, on the convex side, the charge density distributions during the time transition show the different distributions characteristics, indicate that the location of peak shifts from Point 3 to Point 4, as shown in Figure 9b and 10b. From these results, the time constant τ of the charge density on the solid insulator from DC-on to DC steady-state depends on the location of the epoxy-spacer surface. Especially, the growth of charge density at Point 3 on the convex side is remarkable, where the electric field in SF_6 gas is concentrated at DC-on, as shown in Figure 7.

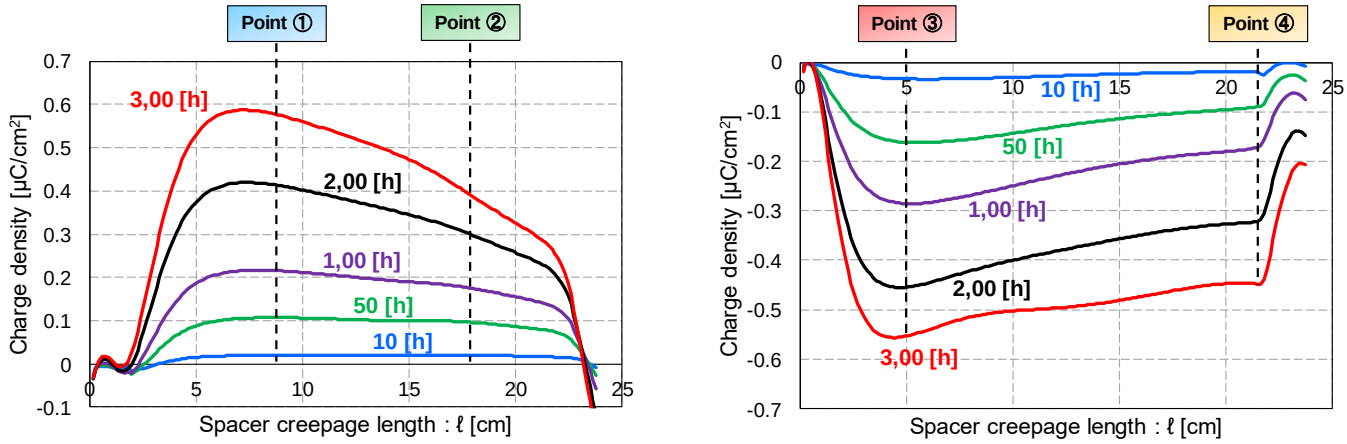

(a) Concave side (b) Convex side

Figure 10. Time transition characteristics of charge density distributions along spacer creepage length ℓ under gas conductivity dominant conditions ($\varepsilon_{EP}/\varepsilon_{gas}$ = 6/1, σ_{EP}/σ_{gas} = $10^{-17}/10^{-16}$ = 0.1, +DC 100 kV application).

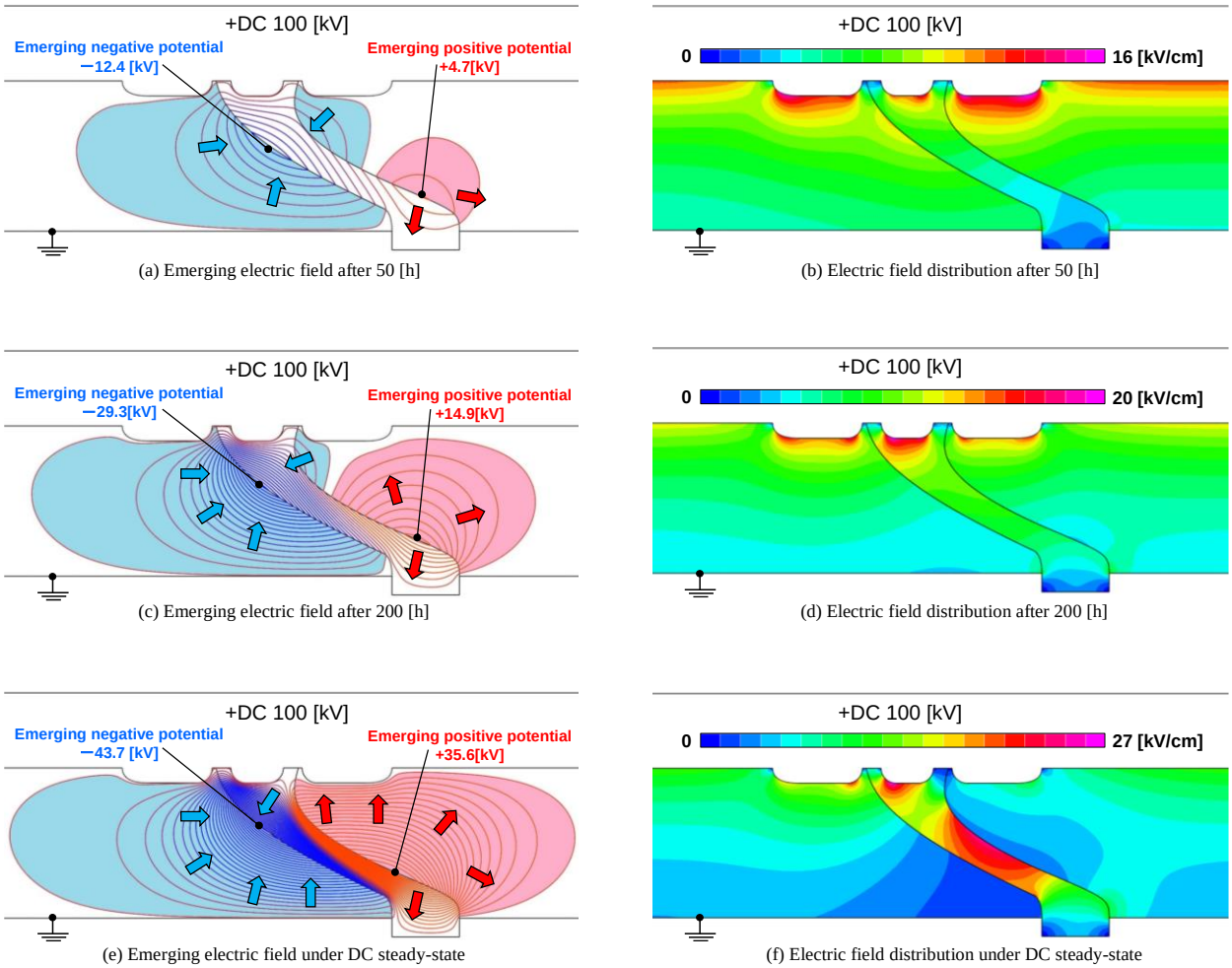

(a) Emerging electric field after 50 [h]
(b) Electric field distribution after 50 [h]
(c) Emerging electric field after 200 [h]
(d) Electric field distribution after 200 [h]
(e) Emerging electric field under DC steady-state
(f) Electric field distribution under DC steady-state

Figure 11. Time transition of emerging electric field due to accumulated charges on solid spacer and resultant electric field distributions in DC-GIS under gas conductivity dominant conditions ($\varepsilon_{EP}/\varepsilon_{gas}$ = 6/1, σ_{EP}/σ_{gas} = $10^{-17}/10^{-16}$ = 0.1, +DC 100 kV application).

4.3 TIME TRANSITION CHARACTERISTICS OF EMERGING ELECTRIC FIELD DUE TO ACCUMULATED CHARGE

Figure 11 shows the time transition of the emerging electric field due to the accumulated charges on the solid insulator and resultant synthetic electric field distributions in an actual insulating spacer model. From these figures, the electric field due to negative accumulated charges on the convex side emerges more than the electric field due to positive accumulated charges on the concave side. This phenomenon can be explained by the remarkable evolution of negative charges at Point 3 in Figure 10a. The electric field stresses in SF_6 gas on the HV conductor shield surface are enhanced by the emerging electric field due to negative accumulated charges on both the concave and convex sides. Finally, the emerging electric field due to positive accumulated charges emerges late on the concave side.

Figure 12 shows the time dependent characteristics of the electric field stresses in SF_6 gas during time transition from DC-on to 300 [h] on the HV electrode shield surface under both gas and solid-dominant conditions. From this figure, in the case of solid-dominant conditions ($\sigma_{EP} > \sigma_{gas}$), the time evolution of electric field stresses at each points in SF_6 gas show little change.

On the other hand, in the case of gas-dominant conditions ($\sigma_{EP} < \sigma_{gas}$), the electric field stresses in SF_6 gas are greatly dependent on the time transition and the location of the gap space. At DC-on (t = 0 [h]), the electric field stress in SF_6 gas at Point D shows the largest value. On the contrary, after 100 [h], the evolution of the electric field stress in SF_6 gas at Point C can be recognized with peak value. Finally, the electric field distributions are determined by the accumulated charge on the epoxy-spacer surface, and the electric field stresses at Points D and C are relaxed, and the electric field stress at Point B shows the highest value. These time and gap space dependent characteristics can be explained by the above discussions about the emerging electric field due to the accumulated charges on the solid insulator.

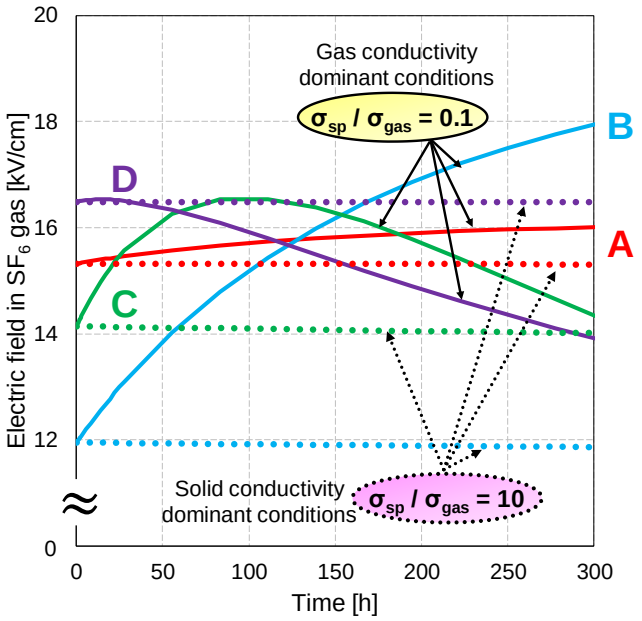

Figure 12: Time and space dependent characteristics of electric field stress in SF_6 gas during time transition from DC-on to 300 [h] on HV electrode surface at points A - D ($\varepsilon_{EP}/\varepsilon_{gas}$ = 6/1, $\sigma_{EP} = 10^{-17}$, $\sigma_{gas} = 10^{-16}$ and 10^{-18} [S/m], +DC 100 kV application, gas conductivity dominant conditions: σ_{EP}/σ_{gas} = 0.1, solid conductivity dominant conditions: σ_{EP}/σ_{gas} = 10).

As a result, we quantitatively clarified that the time transition characteristics of the electric field stress in SF_6 gas are dependent on the location of the gap space based on charge activity. In addition, the location of the maximum electric field stress in SF_6 gas shifts and the most severe condition emerges through the charging process on the epoxy-spacer surface during the time transition from DC-on to DC steady-state.

5 CONCLUSIONS

In this paper, the time and space transition characteristics from DC-on to DC steady-state of the HVDC electric field stress in SF_6 gas and accumulated charges on the epoxy-spacer were investigated in gas-solid composite insulation systems. The following conclusions were quantitatively addressed:

1. The time transition characteristics of the DC electric field and charge density distributions are highly dependent on the electric conduction characteristics in the gap space. This means that the identification of the source of charge carrier, such as electron emission from the conductor surface, partial discharges and so on, is important. Thus, the conductivity values and the local conductivity in the gap space could be critical for DC electrical insulation performance.
2. Under non-uniform electric field in DC composite insulation systems, the time constant τ of electric field formation from DC-on to DC steady-state highly depends on the non-uniformity factor η and location of the gap space in the electrode configurations. The time constant τ would not be a uniform value but different depending on the location in the gap space under non-uniform electric field. Moreover, we clarified that the locations with higher electric field stress in the gap space have the shorter time constant τ of electric field formation.
3. The time transition characteristics of accumulated charge on solid insulators would determine the DC electric field distributions in composite insulation systems. Accordingly, we found that the maximum electric field stress may appear in between initial DC-on and final DC-steady state based on the time transition of emerging electric field due to accumulated charge, depending on the locations and electric field concentrations in the gap space.

REFERENCES

[1] O. Kuhn, P. Menke, R. Zurowski, T. Christ, S. Seman, G. Giering, T. Hammer and D. Imamovic, "2nd generation DC grid access for offshore wind farms: HVDC in an AC fashion", Cigre Session 46, B3-110, 2016.

[2] M. Hering, J. Speck, K. Backhaus, S. Großmann and U. Riechert, "Capacitive-resistive Transition in Gas Insulated DC Systems under the Influence of Particles on the Insulator Surface", *19th Int. Symp. H. V. Eng.*, 2015, No. 157.

[3] H. Okubo, R. Nakane and K. Okamoto, "Partial Discharge Inception Characteristics in Air with Solid Dielectrics under HVDC and Polarity Reversal Conditions", *Annu. Rep. IEEE Conf. Electr. Insul. Dielectr. Phenom.*, 2018, pp.481-485.

[4] F. Messerer, M.Finkel and W. Boeck, "Surface Charge Accumulation on HVDC-GIS-Spacer", *IEEE Int. Symp. Electr. Insul.*, 2002, pp.421-425.

[5] A. Winter and J. Kindersberger, “Transient Field Distribution in Gas-Solid Insulation Systems under DC Voltages”, IEEE Trans. Dielectr. Electr. Insul, Vol. 21, pp.116-128, 2014.
[6] B. Lutz, K. Juhre and D. Imamovic, “Long-term Performance of Solid Insulators in Gas Insulated Systems under HVDC Stress”, *19th Int. Symp. H. V. Eng.*, 2015, No. 530.
[7] T. Yasuoka, Y. Hoshina, M. Shiiki, M. Takei, A. Kumada and K. Hidaka, “Insulation Characteristics in DC-GIS: Surface charge phenomena on epoxy spacer and metallic particle motions”, Cigre Session 47, D1-103, 2018.
[8] M. Schueller, U. Straumann and C. M. Franck, “Role of Ion Sources for Spacer Charging in SF6 Gas Insulated HVDC Systems”, IEEE Trans. Dielectr. Electr. Insul, Vol. 21, pp. 352-359, 2014.
[9] T. Vu-cong, L. Zavattoni, P. Vinson and A. Girodet, “Surface Charge Measurements on Epoxy Spacer in HVDC GIS/GIL in SF_6”, *Annu. Rep.IEEE Conf. Electr. Insul. Dielectr. Phenom.*, 2016, pp. 93-96.
[10] R. Nakane, K. Takabayashi, K. Kato and H. Okubo, “Electric Field Analysis and Electrical Insulation Performance for Gas-solid Composite Insulation in HVDC-GIS”, *20th Int. Symp. H. V. Eng.*, 2017, No. 247.
[11] A. Knecht, “Das Isolationssystem Schwefelhexafluorid-Feststoffisolator bei Gleichspannungsbelastung”, Doctoral Thesis, ETH Zürich, Switzerland, 1984.
[12] J. Kindersberger and C. Lederle, “Surface Charge Decay on Insulators in Air and Sulfurhexafluorid – Part I: Simulation”, IEEE Trans. Dielectr. Electr. Insul, Vol. 15, pp. 941-948, 2008.
[13] M. Tschentscher and C. M. Franck, “Conduction Processes in Gas-Insulated HVDC Equipment: From Saturated Ion Currents to Micro-Discharge”, IEEE Trans. Dielectr. Electr. Insul, Vol. 25, pp. 1167-1176, 2018.
[14] K. Takabayashi, R. Nakane, K. Kato and H. Okubo, “High Voltage DC Partial Discharge and Flashover Characteristics with Surface Charging on Solid Insulators in Air”, IEEE Electr. Insul. Mag., Vol. 34, No. 5, pp.18-26, 2018.

Ryuichi Nakane was born in Gifu, Japan in 1994. He received a M.S. degree in electrical engineering from Aichi Institute of Technology, Japan in 2019. He is currently a Ph.D. candidate of Nagoya University, Japan. He is a student member of IEE of Japan and IEEE.

Naoki Hayakawa (M’90) was born on September 9, 1962. He received a Ph.D. degree in 1991 in electrical engineering from Nagoya University. He has been at Nagoya University since 1990, where he is presently a Professor in the Department of Electrical Engineering. From 2001 to 2002, he was a guest scientist at the Forschungszentrum Karsruhe, Germany. Prof. Hayakawa is a member of IEEE and IEE of Japan and CIGRE.

Hitoshi Okubo (M’81) was born on 29 October 1948. He received the Ph.D. degree in 1984 in electrical engineering from Nagoya University, Japan. He joined Toshiba Corporation, Japan in 1973 and was a manager of the Toshiba high voltage laboratory. From 1976 to 1978 he was at the RWTH Aachen, Germany and the TU Munich, Germany. In 1989, he became an Associate Professor of Nagoya University in the Department of Electrical Engineering, and in 1991 a Professor of Nagoya University in the Department of Electrical Engineering and Computer Science. In 2013 he became a Professor in the Department of Electrical Engineering and Electronics, Aichi Institute of Technology (AIT), Toyota, Japan. In 2011 he was a president of IEE of Japan (IEEJ). He is a member of IEEE, VDE, CIGRE and IEEJ.